de Boer, W.F., L. Rydberg & V. Saide (2000). The influence of tidal currents on an intertidal ecosystem at Inhaca Island...

W. F. de Boer
Wageningen University & Research

Hydrobiologia **428:** 187–196, 2000.

Tides, tidal currents and their effects on the intertidal ecosystem of the southern bay, Inhaca Island, Mozambique

Willem F. de Boer[1,2]*, Lars Rydberg[3] & Victor Saide[4]
[1]*Departamento de Ciências Biológicas, Universidade Eduardo Mondlane, C.P. 257, Maputo, Mozambique*
[2]*Address for correspondence: Bureau Buitenland, RUG, Postbus 72, 9700 AB Groningen, The Netherlands*
Fax: +31-50-3635380
[3]*Department of Oceanography, University of Gothenburg, P.O. Box 460, 40530 Gothenburg, Sweden*
[4]*Departamento de Física, Universidade Eduardo Mondlane, C.P. 257, Maputo, Mozambique*

Received 25 February 1999; in revised form 25 February 1999; accepted 22 January 2000

Key words: tide, current, sediment, flow, mangrove, ebb, flood

Abstract

Sediment characteristics and tidal currents were studied in the 1500 ha intertidal area south of Inhaca Island, Mozambique. The tide is semi-diurnal with a range at spring of about 3 m. The area connects directly to the ocean through the Ponta Torres Strait and (indirectly) through several narrow tidal channels ending up in Maputo Bay. Velocities of up to 0.75 m s^{-1} were measured in the Ponta Torres strait. After Low Water, Indian ocean water starts entering the tidal flats, while entrance from the Maputo Bay side is delayed by one to several hours. With only one tide gauge and one current meter at hand, we found indications of a higher mean sea level on the oceanic side (probably due to ocean wave set up) and a mean flow in the Ponta Torres Strait directed towards Maputo Bay. A storm from the SW had a particularly strong influence on the sea level of Maputo Bay, and for a period of a few days the current flowed constantly towards Maputo Bay. Measurements in the innermost Saco channel indicated higher velocities during ebb than during flood. The resulting residual current will increase sedimentation in the bay, a process which is confirmed by aerial photographs and could be linked to the sanding of the coral reefs and the mangrove extension in the area. Extensive sandbanks are situated around both inlets as a result of the higher current velocities in these areas, thereby inhibiting the settlement of finer sediments and organic matter. Where the two flows meet, formation of mudflats and seagrass beds are favoured. Mudflats are found mainly below High Water Neap, exposed only during spring tides. This longer inundation period favours the settlement of finer material and organic matter. The area and location of the substrates have great influence on the richness and abundance of the benthic fauna, as grainsize and organic matter have been correlated with richness and abundance in other studies.

Introduction

That tides and tidal currents have an impact on the ecosystem structure of shallow bays, basically through the grainsize distribution, is widely accepted. Grainsize of the substrate is negatively linked to abundance and diversity of benthic species (Guerreiro et al., 1996; Raffaelli & Hawkins, 1996; Borzone et al., 1996; Bell et al., 1997). Seagrass beds, for instance rich in associated benthic fauna and fish, are confined to areas with finer sediments (Shi & Chen, 1996). Tidal currents dominate the sedimentation and erosion processes taking place on daily time scales and thereby also affect the nutrient budgets (e.g. Mohammed & Johnstone, 1996; Kitheka et al., 1996). A large difference in water visibility between neap and spring periods illustrates the capacity of the tidal currents to redistribute and export sediments. The physo-chemical properties of the sediment, such as temperature, salinity and oxygen conditions, are also influenced by tidal currents (Day et al., 1989; Hart & Sly, 1992). Tidal asymmetries and residual circulation influence nutrient balances and

* Author for correspondence

sediment loads (Wallin & Håkanson, 1992; Aldridge, 1997; Bowers & Al-Barakati, 1997; Kitheka, 1997; Furukawa et al., 1997).

A basic knowledge of tides and tidal circulation is thus a prerequisite in understanding the intertidal ecosystem of a shallow bay. One of many examples of such an intertidal area is the southern bay of Inhaca Island in Mozambique. The bay is an important fishing ground for the local community. Fish, shellfish and crabs are caught by people in considerable quantities (De Boer & Longamane, 1996). The area is visited by a large number of shorebirds, and palearctic migrants are abundant in summer (De Boer & Bento 1999). The tides and tidal currents in the southern bay were studied, using a tide recording gauge and a current meter. Estimates of the tidal currents were also made with drifters, all with the aim of understanding how the tides influence the ecosystem and affect the distribution of different substrate types of this shallow bay.

Description of sites studied

Inhaca Island is situated on the Mozambican coast, north of the Manchangulo Peninsula. It is separated from land by the short, narrow and deep Ponta Torres Strait which connects the Indian Ocean to Maputo Bay (Figure 1). The strait is kept open by strong oceanic wave action and tidal currents, but its shape seems to change even on short time scales. To the west of Ponta Torres Strait and south of Inhaca are vast tidal flats with a total area of 300 ha. Several narrow and shallow tidal channels appear in this area. These channels connect the area to Maputo Bay and the Indian Ocean (Figure 1). The northern part of the tidal flats, named the southern bay of Inhaca (total area 1540 ha, Figure 1), is delimited by a straight line from Ponta Punduine to Ponta Torres. In this bay, two areas were investigated in detail, the Saco and the Banco.

The nearby Maputo harbour has a tidal range of about 3 m at spring. The climate is a mixture of tropical and subtropical, partly influenced by the SE trade wind, and a northerly monsoon, but also occasionally by strong and cold SW winds or cyclones from the NE. The winter (April–September) is usually cold and dry, while the summer (October–March) is warm and rainy. The mean annual rainfall is 884 mm.

Information regarding Inhaca's intertidal ecology can be found in Kalk (1995), Guerreiro et al. (1996), and De Boer & Longamane (1996). The classification of the five substrate types (Figures 1b and 2) comprises mangroves, sandbanks, mudflats, seagrass beds and channels (Table 1). Mangrove forests fringe the bay. The sandbanks have the highest percentage of coarse sand and have a low silt and fine sand percentage. The percentage of organic matter on the sandbanks is the lowest for the area. The higher lying parts of mangroves and sandbanks are exposed during MHWN tides. The mudflats are not exposed during MLWN tides and have a relatively high percentage of silts, fine sands and organic matter. Seagrass beds can be found in the central part of the bay with the highest percentage of silts and fine sands. *Zostera capensis* is the most abundant seagrass species. The whole area is exposed during ELWS, except for the tidal channels.

Materials and methods

The tidal current within the creeks were studied by use of Spherical Floating Devices (SFDs), in this case oranges, which were set out at high tide in the Saco and at low tide at Ponta Punduine and Ponta Torres. They were traced by boat during periods of 6 h. Experiments were carried out on 3 days at neap tide in August 1997. The wind speed during these days was low. The SFDs, 120 per location, were wrapped in aluminium foil, in brown tape or left untreated to distinguish between three different batches.

Current velocities directly above the sediments were measured with a hand-held stream flow meter (type MFP 51) in several locations above the two study areas once every hour during in- and outgoing tides. Current direction was determined with a compass.

In the tidal channels, velocities and sea-levels were measured with self-recording instruments, a current meter (Sensordata SD-6000) and a tide gauge (MicroTide). The recording interval was set to 10 min. The tide gauge and current meter were deployed at three different locations; in the Ponta Torres Strait, in the interior of the Saco and in the Banco channel (Figure 1b), a few days on each position. In addition, the tide gauge was deployed for a longer period close to Ponta Torres. All these measurements were carried out in December 1996 and January 1997.

Analysis

Differences in current velocity and direction were tested with a trigonometric analysis, the Watson-Williams test and a two-tailed binomial test of Zar

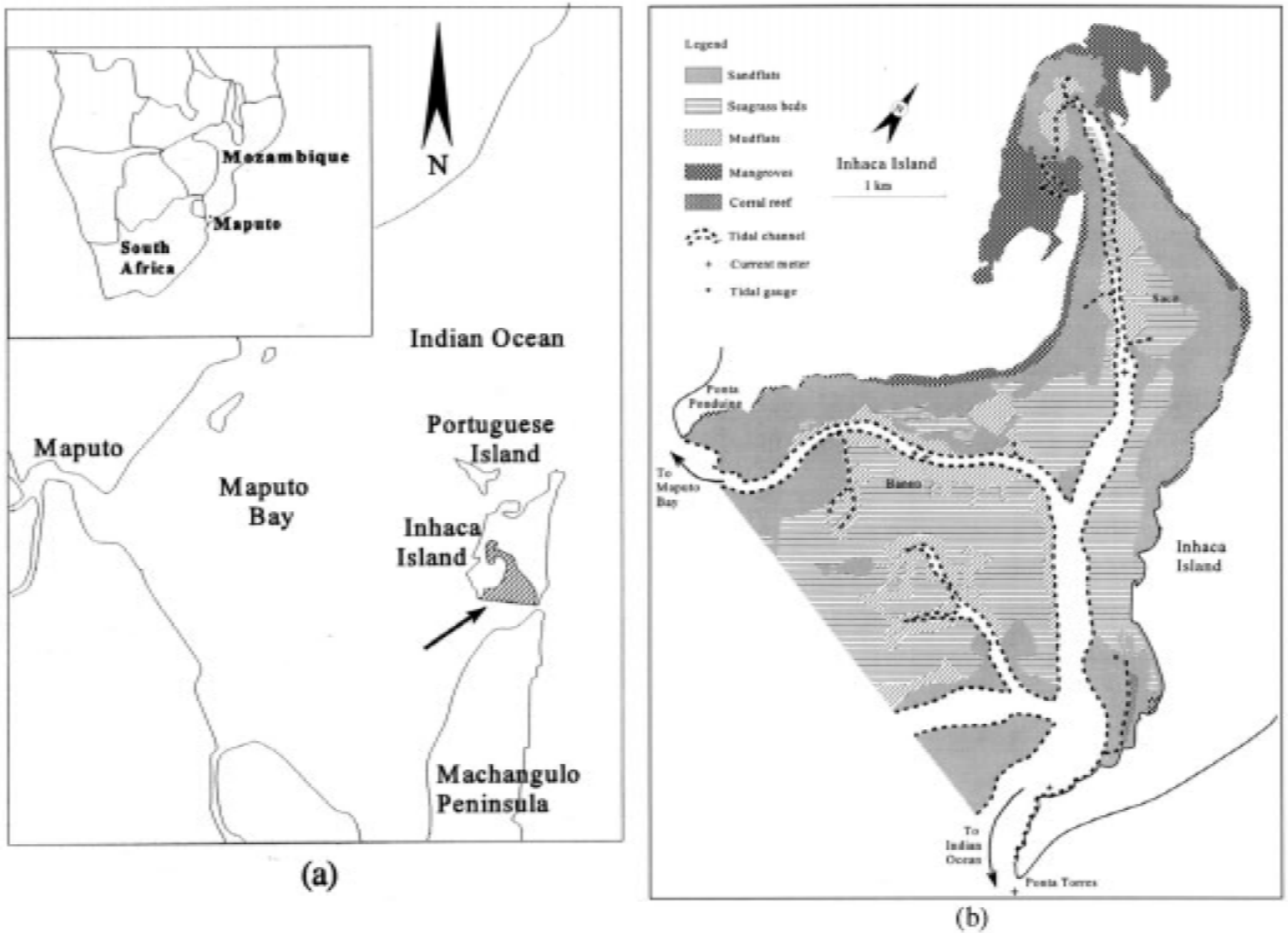

Figure 1. (a) The location of the study area , and (b) the distribution of the substrate types within the southern bay of Inhaca with the two study areas: the Saco and Banco. The locations of tidal gauge (∗) and current meter (+) are indicated.

Table 1. Relative height of the substrates, percentage of the substrate exposed during MLWN tides, mean exposure time during spring tides and substrates' composition: percentage organic matter and percentage silt and coarse sand

	Relative height	Exposed during MLWN	Exposure time	Organic matter	Grainsize	
	m	%	min	%	% silt and fine sands	% coarse sand
Mangroves	0.85–2.60	100	400	1.3	4.6	3.2
Sandbanks	0.60–1.20	100	320	0.5	5.5	4.0
Seagrass beds	1.10–1.60	100	260	1.4	7.9	1.5
Mudflats	0–0.80	20	200	1.5	11.7	2.0
Channel	0–0.70	20	190	1.4	7.8	1.9

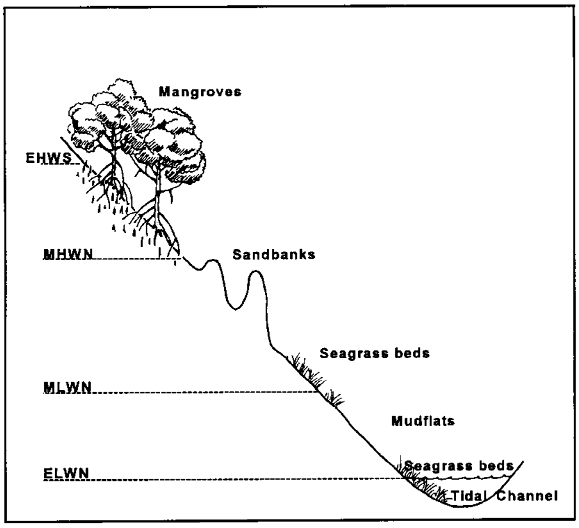

Figure 2. Relative position and height of the different substrates in relation to tide.

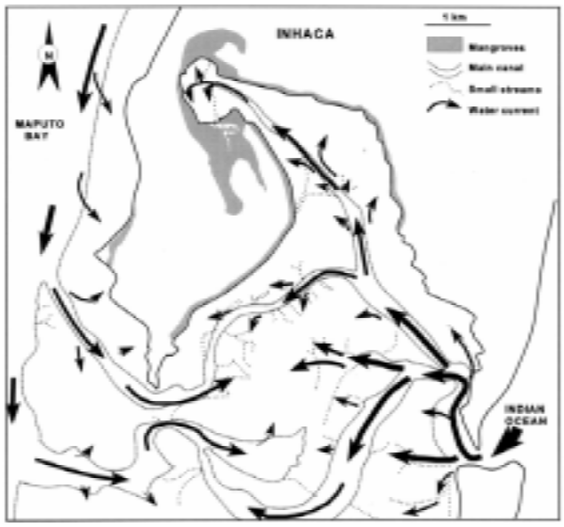

Figure 3. The current direction and relative velocity of incoming currents after low water as registered on 14–15/8/1997.

(1984). Harmonic analysis, following Franco (1981), was used for computation of the tidal constituents (M_2 and S_2). The tidal (volume) flow was estimated with a vector analysis (current velocity × current duration × cross-section area). T-tests were used to test for differences between means.

Results

The flood currents at neap tide, over a period of 6 hours after low water, are illustrated in Figure 3. Water from Maputo Bay started filling the southern bay two hours after low tide, in contrast to the current at Ponta Torres where filling starts immediately. The exposure pattern of the tidal flats during spring tide (deduced from aerial photography and tidal flows) is illustrated in Figure 4. The tidal flats around Ponta Torres were inundated first, the north-western part of the Banco and the tidal flats around the channel to the Saco are only flooded afterwards.

Average current directions and velocities in the Banco area, as observed with the flow meter, are given in Figure 5. During flood, the current directions corresponded to the orientation of the nearby channel. During ebb, currents were significantly different from flood currents minus 180° (F=116.232, df=1,55, p<0.02), and were more orientated towards the channel. This pattern indicates that flood currents fill the bay over a large cross-section of the bay, whilst ebb currents first flowin the direction of the nearby channels before leaving the bay.

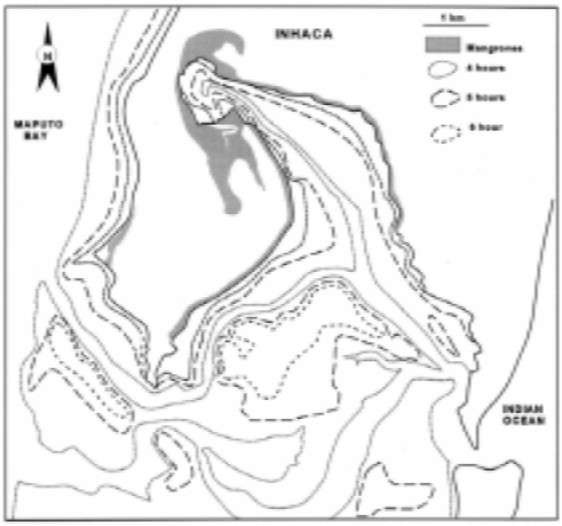

Figure 4. The total exposure time of intertidal flats during low water spring tides.

The marigram from Ponta Torres, shown in Figure 6, indicates a pure semi-diurnal tide with a form factor, F=0.07, only. Harmonic analysis of the relatively short period give spring and neap tidal ranges of 2.2 m and 0.7 m, respectively, surprisingly low compared to the tides in Maputo harbour (see 'Discussion'). The maximum range was less than 3 m. Ebb currents lasted on average 379 min, 15 min longer than flood currents (F=19.661, df=1,86, $p<0.0001$).

The tidal currents in the Ponta Torres Strait, observed over 5 days, are shown in Figure 7. The maximum velocity depended on two major factors. First, it increased with larger tidal range. Furthermore, a maximum of 0.75 m s^{-1} was seen during inflow of Indian Ocean waters, which decreased to only 0.50 m s^{-1} during outflow. Lower current speeds during outgoing tides were compensated by an increase in current duration. Average duration of outgoing tidal currents was approximately 400 min, statistically longer than the shorter bout of incoming ocean water, equal to 348 min (t=3.66, df=8.2, $p<0.01$). Nevertheless, the water volume entering the bay through Ponta Torres was 65% larger than the volume leaving during outgoing tides (t=-2,73, df=10.6, $p<0.025$), indicating an average through flow towards Maputo Bay.

The tidal currents in the Saco channel are depicted in Figure 8. Here, ebb and flood duration were equal (365 min *versus* 376 min). During ebb, the highest velocities were measured near LW, with velocity maxima of 0.70 m s^{-1}. Also at flood, the highest velocities (0.50 m s^{-1}) appeared just before HW. These velocit-

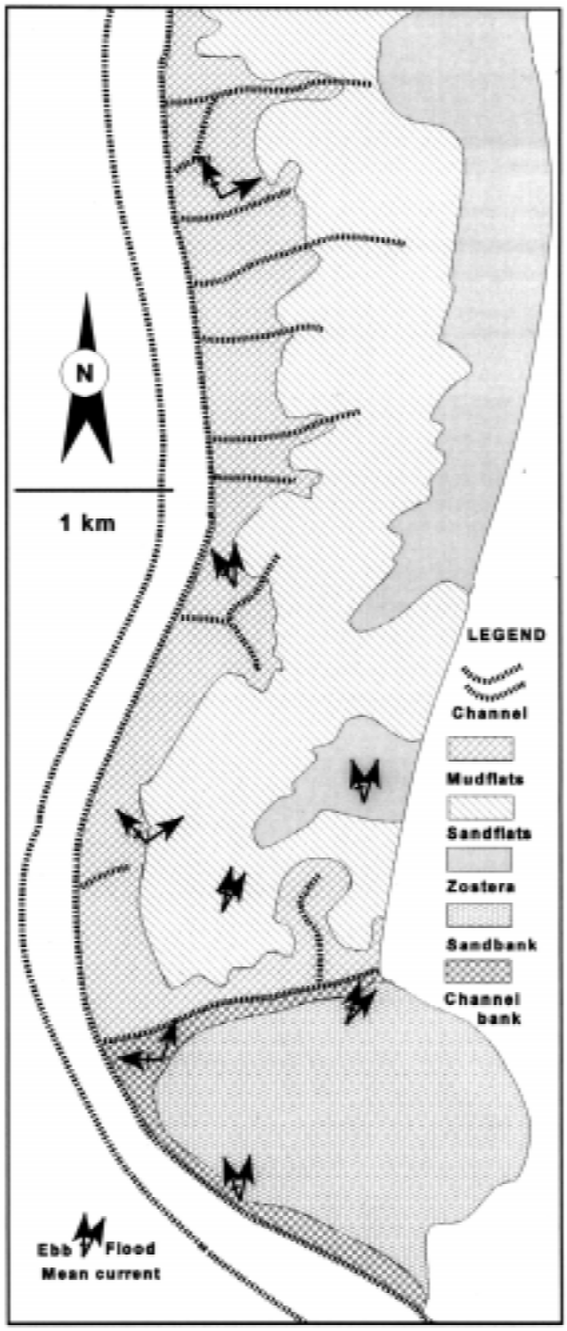

Figure 5. Mean current directions of ebb and flood currents over the substrate types in the Banco area (for location see Figure 1b). The two arrows at the left give the average ebb and flood directions for the area as a whole.

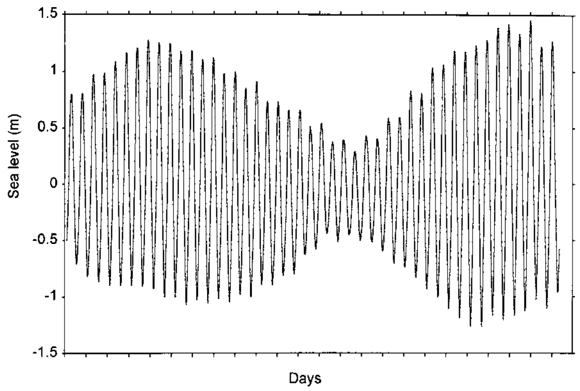

Figure 6. Sea level changes (m) during a spring and a neap tidal cycle at Ponta Torres, 23 days from 21/12/1996 to 12/01/1997.

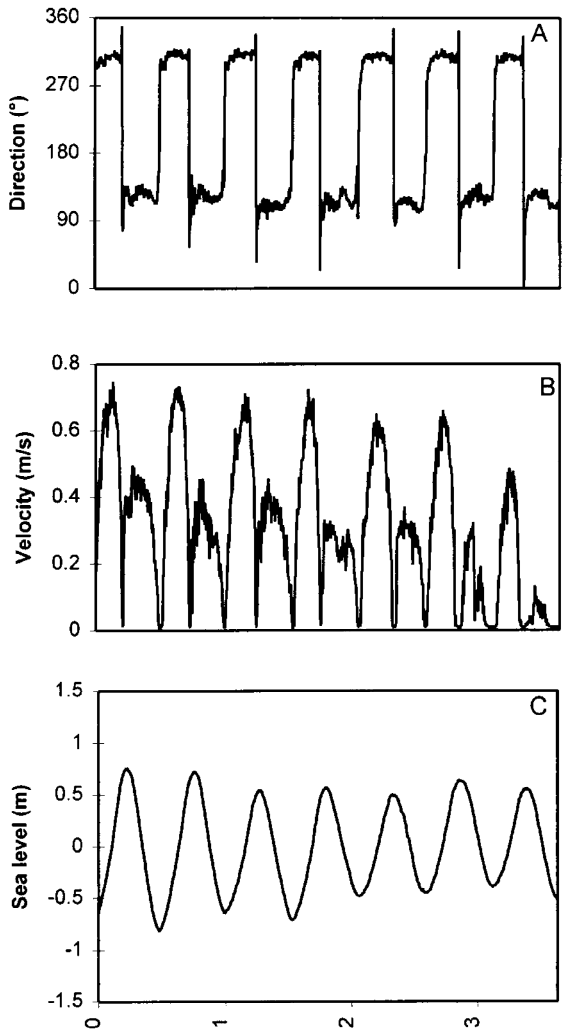

Figure 7. (a) Current direction degrees from north, (b) water current velocity (m s^{-1}), and (c) sea level (m) over 3 days in the Ponta Torres Strait.

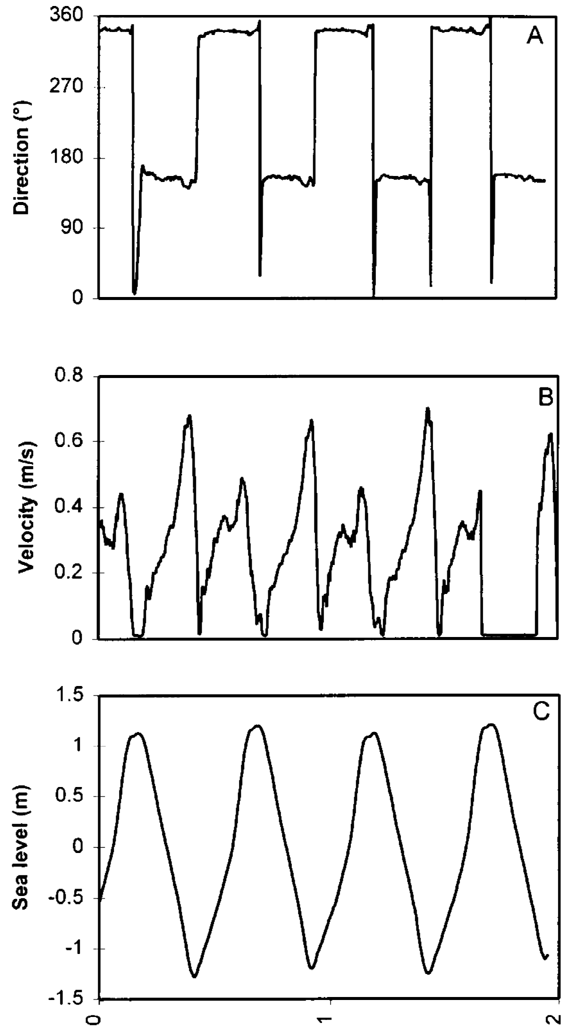

Figure 8. (a) Current direction in degrees from north, (b) water current velocity (m s^{-1}), and (c) sea level (m) in the Saco over two days of spring tide.

ies coincided with a rapid sea level change, which is illustrated by the steeper slopes of the sea-level curve. Ebb currents had higher velocity maxima. During ebb, the water volume through the channels was 28% larger than that of flood current.

Figure 9 shows the tidal current measurements in the Banco channel. Contrary to the Saco, flood current had higher velocities compared to ebb currents, but current velocities were equal to the Saco and Ponta Torres. An interesting pattern is seen in Figure 9, because of the edge effects of a cyclone passing east of Inhaca. Current direction changed, first the duration of the outgoing water current was shortened from 220 min in the first cycle to 165 in the second and 125

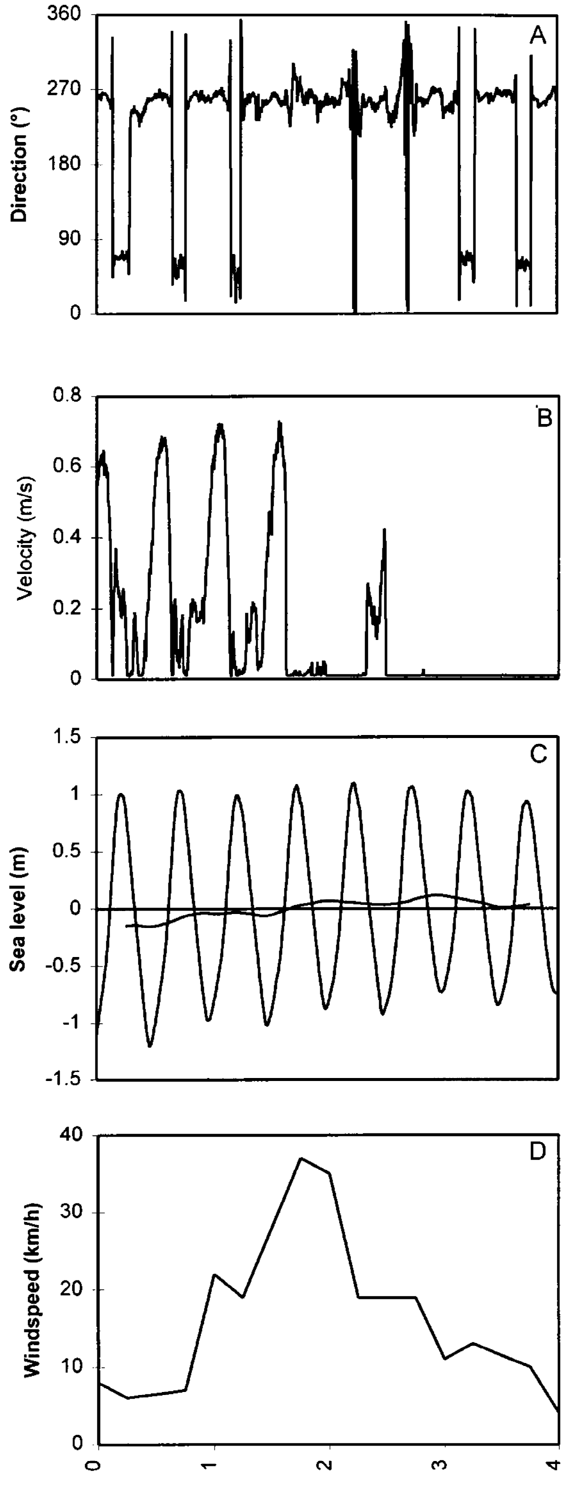

Figure 9. (a) Current direction in degrees from north, (b) water current velocity (m s^{-1}), (c) sea level (m), and (d) windspeed (km h^{-1}) in the Banco over four days of spring tide with heavy weather in the middle of the sampling period. The line in C represents the one-tidal cycle running average (−6 h – +6 h).

min in the third. After three tidal cycles, it completely disappeared for 24 h, and the strong south-westerly wind generated a stable current towards the bay and consequently masked tidal currents. MSL was 0.3–0.4 m higher during the cyclone than at the beginning and end of the sampling period. The normal pattern of current changes was restored at the end, with outgoing current duration still at 31% of the duration of incoming waters.

The neap tide data available for the Banco showed that the currents were smaller (< 0.40 m s^{-1}) than spring currents and that the duration of the ebb current was longer: 315 min for neap tides, compared to around 200 min during normal spring tides. Moreover, considerable periods with very small current velocities (< 0.05 m s^{-1}) were registered during neap tides. Current velocity data for neap tides in the Saco area are not presented as algae clogged the rotor.

Discussion

The tides, according to the harmonic analysis of the tide gauge measurements, are semi-diurnal with a spring and neap tidal range of 2.2 m and 0.7 m, respectively. The volume differences between spring and neap tides can be estimated from water depth (Figure 1 and Table 1) and bay area (15 400 ha), and are 26.10^6 m^3 for spring and 16.10^6 m^3 for neap tides. The LW volumes were 4.10^6 m^3, and 7.10^6 m^3, respectively. Hence, the differences between HW and LW water volumes, the tidal prisms, are 22.10^6 m^3 for spring tide and 9.10^6 m^3 for neap tide. A conservative estimate of the water volume entering the bay at Ponta Torres (data from Figure 7) is 770 m^3 s^{-1}, based on a mean depth of 10 m, a width of 200 m and a mean velocity of 0.38 m s^{-1}. Incorporating current duration (348 min), a total of 16.10^6 m^3 is estimated at entering the bay during flood through the strait. Part of this water covers the intertidal areas outside the southern bay. Comparing the water volume necessary to fill the bay and the volume entering the bay at Ponta Torres, the conclusion can be drawn that the bulk of the water filling the southern bay comes from the Indian Ocean. Water from Maputo Bay enters the area south of Inhaca on a basin-wide scale. This implies relatively efficient mixing with oceanic water. Thus, the outflow during ebb at Ponta Torres may include a considerable amount of Maputo Bay water. Assuming that the nutrient load of the estuarine Maputo Bay water is larger than the Indian Ocean waters (see Kitheka et al., 1996), the conclusion can be drawn that the most important external nutrient source for the southern bay is probably the Maputo Bay flood current. Both the calculus of the different water volumes and Figure 3 indicate that the eastern side of the southern bay, including the interior of the Saco, is filled mainly by the clearer ocean waters, whilst the south-western part is mainly filled by currents from Maputo Bay.

The ebb period at Ponta Torres was slightly longer than the flood period. The ebb flow was relatively small (330 m^3 s^{-1}, with a mean velocity of 0.17 m s^{-1}), indicating that an average of 8.10^6 m^3 left the bay through Ponta Torres during ebb. Apparently, the water volume entering the southern bay through Ponta Torres (16.10^6 m^3) was larger than the volume leaving. Hence, there is a net flux from the Indian Ocean towards the Maputo Bay of 8.10^6 m^3 per tidal cycle. This flow pattern can be sustained only by a lower sea level on the Maputo Bay side at the start of the flood. This is sustained some time while the flow in the tidal channel is towards west for several hours. Later, however, the sea level difference approaches zero and the large opening towards Maputo Bay allows for a larger flow into the Banco area during the second half of the flood period.

The differences between neap and spring tides at the Banco is explained by the flooding pattern of two different currents arriving from different directions, the Indian Ocean and Maputo Bay. The water currents measured during neap were apparently an effect of the two currents meeting each other and cancelling each other out. Tidal height continued to change but currents were small. The shorter bouts of ebb currents during spring tides at the Banco were caused by the narrow Ponta Torres Strait, which is a physical barrier for the outgoing currents. This effect was smaller during neap tides, when a smaller volume passed the strait and consequently the ebb periods tended to increase. The switching of current direction from flood to ebb (in contrast to water height changes, which is independent of current direction, e.g. compare with Figure 9) took more time during spring tides and consequently decreased the ebb period.

The tidal currents were different during the period when the cyclone passed the area. Southerly storms are expected to rise MSL along the coast of the Indian Ocean because of the Ekman drift. A directly decreasing sea level may be expected within the relatively small and shallow southern bay, because of a wind-drift out from the bay (Figure 9). Both factors tend to increase the sea-level difference between the Ocean and Maputo Bay, thus giving rise to a continuous through-flow towards Maputo Bay.

The maximum currents in the Banco and Saco channels were about 0.70 m s^{-1}. Velocities were influenced by the friction of the surrounding mangrove vegetation (Wolanski, 1992; Furukawa et al., 1997), generating an asymmetrical velocity curve, which was more pronounced in areas closer to the mangroves, such as the Saco.

The incoming currents tended to be faster than the outgoing currents at Ponta Torres. The currents probably also have different sediment loads, suggesting that there is a net output of suspended sediment leaving the southern bay through the Ponta Torres Strait. This mainly depends on differences in sediment load and other factors (e.g. Ferretti et al., 1992; Evans & Håkanson, 1992; Vlag, 1992; Tamminga, 1992; Ke et al., 1996; Edelvang & Austen, 1997).

Another factor which is responsible for a net sediment transport is the different direction of ebb and flood currents above the substrates. The higher currents registered in the Saco area and the calculated higher flux of outgoing water is probably related to the fact that outgoing waters tend to follow the channels rather than incoming waters, a typical feature of shallow mudflats (see Shetye & Gouveia, 1992; Yin et al., 1996). The high ebb velocities indicate that all water leaving the Saco near LW, probably flow through the channel. The water entering the bay during the following flood, apparently showed a tendency to fill the bay not only through the channel but over a wider cross-section of the intertidal area. This is confirmed by the different directions of ebb and flood currents above the substrates at the Banco. The general perpendicular orientation of second-order tidal creeks on the main channel (Figure 1), supports the hypothesis that ebb currents tend to concentrate first in the main channel before leaving the area. The difference in ebb and flood current direction does generate a flood-directed residual current over the intertidal areas (see mean direction in Figure 5), which may be important for net sediment transport (see also Bowers & Al-Barakati, 1997). This residual current would produce sediment accumulation in the direction of the flood current. That the area is silting up was confirmed by aerial photograph interpretation. The total area covered by sandbanks increased by 9% between 1967 and 1989 from 540 ha to 590 ha. In addition, people from the island, and D. Kilburn (pers. com.), who has visited the area several times during the last three decades, have mentioned that the benthic fauna in the interior of the Saco has decreased substantially due to the invasion of sandbanks. Moreover, the sanding of the coral reefs near Ponta Torres and the increase of the mangrove forests in the area also seems linked to this phenomenon (own observation).

The exact location of the instruments is important for obtaining a complete image of the bay's currents, and other sites should also be studied (e.g. at Ponta Punduíne and in the main mangrove channels). Synchronous recordings, including sediment load analysis, should be made at different sites over a longer period of time (see Lane et al., 1997).

The locations of the substrates (Figure 1) can be linked to the morphodynamic influence of tidal currents. Large sandbanks are situated around the two entrances at Ponta Torres, at Ponta Punduine and at Ponta Rasa. The water enters the southern bay with high velocities (Figure 7), enabling the settlement of coarse sand only, because settling rate is faster with increasing particle diameter (the impact law: see McLusky, 1989; Allan, 1995). The sandbanks in the Saco area (Figure 1) are located close to the mangrove channel and the small Saco Strait. These sites experience high water velocities at the end of the ebb currents, which erode the substrates and enable only coarser sediment to settle. The organic matter is consequently low in these substrates (Table 1).

In the area where the Ponta Torres and Maputo Bay currents meet, at a north-south orientated line over the study area (compare Figures 1 and 3), the currents cancel each other out. The smaller water velocities in this central part of the bay enable the settlement of finer material, explaining the central location of the seagrass beds and mudflats in the bay. When the ebb current velocities are still small, just after HW, and during a prolonged period of inundation at neap tides, the mudflats can be formed. The continuous flooding, during neap tides, of these lower lying areas enables the settlement of finer cohesive material and contributes to the formation of the mudflats and seagrass beds with a relatively high %OM. Coarser sandbanks with a low %OM are, therefore, only found in areas where 1. the inundation period it too short for the settlement of finer material, e.g. on relatively higher lying areas, or 2. fast currents inhibit the settlement of silts and OM, e.g. close to in- and outlets of large water volumes. The trapping effect of mangrove and seagrass vegetation is also important in sediment formation. Grainsize is a major factor in determining benthic fauna richness and distribution (Borzone et al., 1996; Guerreiro et al., 1996; Raffaelli & Hawkins, 1996; Shi & Chen, 1996; Bell et al., 1997). Acknowledging the role tidal currents play in sediment transport and settlement and in the distribution of nutrients, the conclusion can be drawn that tidal currents directly determine the structure of the intertidal ecosystem of the intertidal areas at Inhaca.

Acknowledgements

We would like to thank the people of the Marine Biology Station on Inhaca for their hospitality and assistance during the fieldwork. John Largier advised us about SFD design. Several students from the ecology course helped with the current measurements carried out above the substrates. The research has been carried out in the framework of the Deibi project (W.F. de Boer) and the Sarec project (R. Rydberg and V. Saide). We would like to thank our colleagues at Eduardo Mondlane University and especially Herbert Prins for comments on earlier versions of the manuscript.

References

Aldridge, J. N., 1997. Hydrodynamics model predictions of tidal asymmetry and observed sediment transport paths in Morecambe Bay. Estuar. coast. shelf Sci. 44: 39–56.

Allan, J. D., 1995. Stream Ecology; Structure and Function of Running Waters. Chapman & Hall, London: 388 pp.

Bell, R. G., T. M. Hume, T. J. Dolphin, M. O. Green & R. A. Walters, 1997. Characterisation of physical environmental factors on an intertidal sandflat, Manukau Harbour, New Zealand. J. exp. mar. Biol. Ecol. 216: 11–31.

Borzone, C. A., J. R. B. Sousa & A. G. Soares, 1996. Morphodynamic influence on the structure on inter and subtidal macrofaunal communities of subtropical sandy beaches. Rev. chil. Hist. nat. 69: 565–577.

Bowers, C. D. & A. Al-Barakati, 1997. Tidal rectification on drying estuarine sandbanks. Estuaries 20: 559–568.

Day, J. W., C. A. S. Hall, W. M. Kemp & A. Yáñez-Arancibia, 1989. Estuarine Ecology. Wiley & Sons, London: 558 pp.

De Boer, W. F. & C. M. Bento, 1999. The Birds of Inhaca Island, Mozambique. Monoi BLSA Guide N° 22. Birdlife SA, Johannesburg: 76 pp.

De Boer, W. F. & F. A. Longamane, 1996. The exploitation of intertidal food resources in Inhaca bay, Mozambique. Biol. Conserv. 78: 295–303.

Edelvang, K. & I. Austen, 1997. The temporal variation of flocs and fecal pellets in a tidal channel. Estuar. coast. shelf Sci. 44: 361–367.

Evans, R. D. & L. Håkanson, 1992. Measurement and prediction of sedimentation in small Swedish lakes. Hydrobiologia 235/236 (Dev. Hydrobiol. 75): 143–152.

Ferretti, O., I. Niccolai, S. Tucci, M. Setti & F. Immordino, 1992. Transport and distribution of sediments along the Ligurian coasts. Hydrobiologia 235/236 (Dev. Hydrobiol. 75): 17–32.

Franco, A. S., 1981. Tides, Fundamental Analysis and Prediction. IPT, São Paulo: 233 pp.
Furukawa, K., E. Wolanski & H. Mueller, 1997. Currents and sediment transport in mangrove forests. Estuar. coast. shelf Sci. 44: 301–310.
Guerreiro, J., S. Freitas, J. Pereira, J. Paula & A. Macia Jr., 1996. Sediment macrobenthos of mangrove flats at Inhaca Island, Mozambique. Cah. Biol. Mar. 37: 309–327.
Hart, B. T. & P. G. Sly (eds), 1992. Sediment/Water Interactions. Developments in Hydrobiology 75. Kluwer Academic Publishers, Dordrecht, The Netherlands. 743 pp. Reprinted from Hydrobiologia 235/236.
Kalk, M., 1995. A Natural History of Inhaca Island. Witwatersrand Univ. Press, Johannesburg: 394 pp.
Ke, X., G. Evans & M. B. Collins, 1996. Hydrodynamics and sediment dynamics of The Wash embayment, eastern England. Sedimentology 43: 157–174.
Kitheka, J. U., 1997. Coastal tidally-driven circulation and the role of water exchange in the linkage between tropical coastal ecosystems. Estuar. coast. shelf Sci. 45: 177–187.
Kitheka, J. U., B. O. Ohowa, B. M. Mwashote, W. S. Shimbira, J. M. Mwaluma & J. M. Kazungu, 1996. Water circulation dynamics, water column nutrients and plankton productivity in a well-flushed tropical bay in Kenya. J. Sea Res. 35: 257–268.
Lane, A., D. Prandle, A. J. Harrison, P. D. Jones & C. J. Jarvis, 1997. Measuring fluxes in tidal estuaries: sensitivity to instrumentation and associated data analysis. Estuar. coast. shelf Sci. 45: 433–451.
McLusky, D. S., 1989. The Estuarine Ecosystem. Blackie Academic & Professional, London: 215 pp.
Mohammed, S. M. & R. W. Johnstone, 1995. Spatial and temporal variations in water column nutrient concentrations in a tidally dominated mangrove creek: Chwaka Bay, Zanzibar. Ambio 24: 482–486.
Raffaelli, D. & S. Hawkins, 1996. Intertidal Ecology. Chapman & Hall, London: 356 pp.
Shetye, S. R. & A. D. Gouveia, 1992. On the role of geometry of cross-section in generating flood dominance in shallow estuaries. Estuar. coast. shelf Sci. 34: 1–14.
Shi, Z. & J. Y. Chen, 1996. Morphodynamics and sediment dynamics on intertidal mudflats in China (1961–1994). Cont. Shelf Res. 16: 1909–1926.
Tamminga, G. H., 1992. Interpretation of sediment data measured in a former tidal channel Lake Volkerak. Hydrobiologia 235/236 (Dev. Hydrobiol. 75): 107–117.
Vlag, D. P., 1992. A model predicting waves and suspended silt concentration in a shallow lake. Hydrobiologia 235/236 (Dev. Hydrobiol. 75): 119–131.
Wallin, M. & L. Håkanson, 1992. Morphometry and sedimentation as regulating factors for nutrient recycling and tropic state in coastal waters. Hydrobiologia 235/236 (Dev. Hydrobiol. 75): 33–45.
Wolanski, E., 1992. Hydrodynamics of mangrove swamps and their coastal waters. Hydrobiologia 247 (Dev. Hydrobiol. 80): 141–162.
Yin, Y., G. Cheng, S. Fan & Y. Wang , 1996. Morphology and hydrodynamics of tidal channels in Yellow River Delta. In Institute of Marine Geology (ed.), Proceedings of the 30th International Geological Congress, 2. Institute of Marine Geology, Qingdao: 218 pp.
Zar, J. H., 1984. Biostatistical Analysis. Prentice Hall, London: 718 pp.